Research Square

Preprints are preliminary reports that have not undergone peer review.
They should not be considered conclusive, used to inform clinical practice,
or referenced by the media as validated information.

Wood quality and material integrity of wildfire-exposed Cryptomeria japonica evaluated by mechanical grading and multi-scale characterization

Yuta Nakayasu
nakayasu@tohoku.ac.jp

Tohoku University
Kosuke Yamaguchi
Iwate Prefectural Forestry Technology Center
Kayoko Kobayashi
Kyoto University
Yuka Nakagawa
Kyoto University Institute for Chemical Research
Keisho Ri
Tohoku University
Keito Mineo
Kyoto University Institute for Chemical Research
Takaaki Tomai
Tohoku University
Hironori Taniuchi
Iwate Prefectural Forestry Technology Center
Yoshiya Touge
Chiba University

Research Article

Keywords: bark degradation, chemical integrity, Cryptomeria japonica, mechanical grading, wildfire-damaged wood

Posted Date: July 8th, 2026

DOI: https://doi.org/10.21203/rs.3.rs-10084994/v1

License: This work is licensed under a Creative Commons Attribution 4.0 International License. Read Full License

Additional Declarations: No competing interests reported.

Abstract

This study evaluated the post-fire wood quality and material integrity of Japanese cedar (Cryptomeria japonica) recovered approximately three months after the 2025 Ofunato wildfire in Japan. Thirty trees were classified into three visual burn-severity classes based on the height of stem charring. Two 2.1-m logs per tree were processed for longitudinal vibration testing, lamina production, bark-thickness measurement, microscopy, chemical composition analysis, Fourier-transform infrared spectroscopy, wide-angle X-ray diffraction, thermogravimetry, and chlorine analysis. Dynamic log modules and machine-graded lamina modulus showed no monotonic decrease with increasing burn severity. The modal log class was Ef70 in all severity classes, and most of the 711 kiln-dried laminae were assigned to L50–L80 classes; about 99% met the lamina-grade requirements assumed for an E55-F200-equivalent mixed-grade glued-laminated timber layup. Severe burning mainly affected the bark: approximately 75% of bark-thickness measurements in the severe class were below 2 mm, indicating reduced protection against subsequent checking and biodeterioration. In a representative severe sample, microscopy showed retained tracheid cell-wall frameworks, and chemical, spectroscopic, crystallographic, and thermal analyses detected no marked degradation of the remaining internal wood. Chlorine concentrations in tested burned samples did not indicate clear residual salt enrichment relative to regional controls. These results show that prompt mechanical grading, rather than visual charring alone, is essential for reuse decisions, while rapid salvage and processing are needed because bark loss may accelerate post-fire deterioration. These results show that prompt mechanical grading, rather than visual charring alone, is essential for reuse decisions, while further verification of destructive strength, bonding performance, durability, and storage effects is required before final product-level use.

1. Introduction

In recent years, compound fire-weather conditions associated with high temperature, prolonged dryness, and strong wind have intensified concern about extreme wildfires in many parts of the world. In Japan as well, large wildfires are again being recognized as a major social and environmental issue. The wildfire that began in Ofunato City, Iwate Prefecture, on 26 February 2025 was officially extinguished on 7 April 2025 (Fire and Disaster Management Agency 2025). The official forest-damage survey reported a damaged forest area of 3,370 ha and an estimated monetary damage of 5.939 billion yen (Ofunato City 2025). In addition to damage to houses and infrastructure, the event left extensive areas of scorched planted forest on steep coastal slopes, where delayed intervention could create long-lasting safety and recovery problems.

The material consequences of such fires are especially important in Japan because planted forests account for a large share of the national forest resource, and Japanese cedar (*Cryptomeria japonica*) is the major planted conifer species in Japan (Forestry Agency 2025). *C. japonica* is also a major raw material for sawn timber and glued-laminated timber used in housing and public buildings. If wildfire-exposed *C. japonica* is rejected solely on the basis of blackened bark or superficial scorching, a large potentially usable resource may be lost. Conversely, if material is reused without evidence-based evaluation, hidden deterioration could compromise processing efficiency, durability, or structural performance. A practical decision framework therefore requires both mechanical grading and chemical or microstructural examination.

A useful domestic precedent is the Ozaki Peninsula wildfire in 2017 in Kamaishi city, Iwate Prefecture. Following that event, burned conifer logs were salvaged, transported, and utilized as glued-laminated products and other wood materials, including locally symbolic applications (Forest Management Center 2024). At the same time, previous observations of fire-damaged stands indicate that post-fire tree survival and subsequent decline are closely related to the degree of stem scorching, suggesting that the timing of salvage can be critical (Sasa et al. 1989). In steep Sanriku terrain, prolonged abandonment of fire-damaged forest also raises broader concerns related to slope instability, restricted access, and downstream transport of woody debris.

Previous studies from outside Japan suggest that wildfire effects on wood properties depend strongly on heat intensity, residence time, and the degree to which heat penetrates beyond bark and cambium. For post-fire conifers exposed mainly to surface fire, density and stiffness often remain close to those of sound wood, whereas more severe heat exposure can reduce mechanical performance (Bortoletto Júnior and Moreschi 2003; Marttila et al. 2024). Chemical studies likewise indicate that the principal cell-wall polymers may remain largely intact when heating is limited, even though discoloration, extractive redistribution, and surface-zone chemical changes can occur (Barčić et al. 2022; Bortoletto Júnior and Moreschi 2003; Zachar et al. 2025). Under higher temperatures or longer exposure times, however, hemicellulose degradation, cellulose depolymerization, and changes in lignin chemistry become more pronounced (Candelier et al. 2016; Hill et al. 2021; Korkut et al. 2008; White and Dietenberger 2001).

Despite the relevance of these findings, empirical evidence for *C. japonica* from an actual large wildfire remains limited. In particular, there has been little integration of large-sample lamina grading with bark-condition assessment, microscopy of discolored zones, preliminary chemical characterization, and evaluation of possible salt contamination associated with seawater-based fire suppression. This is an important gap because large wildfires have repeatedly occurred in Japan, and their spatial and temporal characteristics have recently been summarized at the national scale (Touge et al. 2024). In the present Ofunato case, concern about seawater-derived chloride deposition was particularly relevant because samples were collected from areas affected by aerial seawater spraying and direct seawater extinguishing, as described in Sect. 2.6. In addition, seawater and lakes provide sufficient water depth, offering advantages for aerial water intake operations. Similarly, during the 2025 Ofunato wildfire, both ground and aerial firefighting units actively utilized seawater for suppression activities. Concerns have therefore extended beyond heat damage alone to include possible chloride residues that could affect processing or service performance.

Another practical bottleneck lies in debarking and preprocessing. Carbonized or loosened bark may alter the efficiency of mechanical debarking and could increase labor or tool wear during log handling, even when the wood substance remains largely sound. Moreover, the economic and institutional conditions of post-fire salvage in Japan mean that material soundness alone does not guarantee implementation. Costs associated with transport, marketing, site management, and plan preparation can still limit recovery and utilization at the owner or operator level.

Against this background, the present expanded manuscript synthesizes current results from the ongoing survey of wildfire-exposed *C. japonica* in Ofunato. This study tested three hypotheses: first, that visual burn severity based on stem charring does not necessarily correspond to reduced log or lamina stiffness after removal of visibly charred surfaces; second, that severe external charring primarily affects the bark and cambial region rather than causing marked degradation of the remaining xylem; and third, that seawater-based fire suppression does not necessarily leave a residual chlorine signal exceeding the regional background level in the tested material. To test these hypotheses, wildfire-exposed *C. japonica* was evaluated by log vibration testing, machine grading of laminae, bark-thickness measurement, microscopy, chemical composition analysis, spectroscopic and crystallographic characterization, thermogravimetry, and chlorine analysis.

2. Materials and Methods

2.1 Overview of the 2025 Ofunato wildfire and study design

Approximately 50% of the burned area consisted of planted forests, while about 44% consisted of natural forests, based on forest-type mapping. The burned area in Ofunato was covered by both planted and natural forests, and the planted forests mainly consisted of conifers such as Cryptomeria japonica and Pinus densiflora (Fire and Disaster Management Agency 2025). The burned area also exhibited considerable spatial variability in burn severity. Figure 1**(a)** shows the difference in the Normalized Burn Ratio (dNBR) derived from Sentinel-2 imagery before and after the wildfire. A severely burned area associated with a large-scale crown fire was identified in the southern part of the study area, while extensive areas were characterized mainly by surface fires with localized intense burning.

The present study focused on *C. japonica* planted forests affected by the 2025 Ofunato wildfire in Iwate Prefecture. The fire burned across a wide coastal-mountain interface, where delayed salvage would have implications not only for timber recovery but also for access, slope management, and regional recovery. The survey was organized to address a practical question frequently raised by local stakeholders: whether partially scorched *C. japonica* stems should be discarded as damaged material or can still be graded and processed as engineering-wood feedstock.

Because fire-suppression conditions varied spatially and included concern about possible seawater-derived chloride deposition, the assessment combined three layers of evidence: (i) mechanical grading of whole logs and processed laminae, (ii) microscopy and preliminary chemical analyses of representative discolored zones, and (iii) chlorine measurements for bark and sapwood collected from representative burned material.

In addition to the logs used for mechanical testing, disks were cut at several stem heights for bark-thickness measurement and chemical sampling. The current draft emphasizes the analyses for which interpretable results are already available.

2.2 Burn-severity classification and field sampling

Field sampling was carried out on 2–4 July and 9 July 2025. Trees were classified visually into three burn-severity classes according to the maximum height of bark charring on the standing stem: low severity (Fig. 1b), moderate severity (Fig. 1c), and severe severity

(Fig. 1d). In operational terms, low-severity trees showed partial charring near the butt (approximately below 1.5 m), moderate-severity trees showed stem charring up to roughly 5 m, and severe-severity trees were charred from the stem base to the crown. Photographs of the felled trees classified by burn severity are shown in **Figs. S1–S3**. This classification was adopted as a practical field indicator of heat exposure and is consistent with the severity framework used in the related local reports.

Ten C. japonica trees were felled in each burn severity class. Each tree was processed into two approximately 2.1-m logs, namely a butt log and a second log, representing the lower and upper stem positions, respectively. These logs were used for mechanical evaluation, yielding 20 logs per class and 60 logs in total. Burn severity was classified as low when partial burning was confined to within 1.5 m of the stem base, moderate when partial burning extended to within 5 m of the stem base, and severe when continuous burning was observed from the trunk to the branches. In addition, 50-mm-thick disks were collected for bark-thickness measurement, microscopic observation, and chemical analysis.

Disks were additionally taken from the stem for bark-thickness assessment and for selection of representative discolored zones. Low- and moderate-severity material was sampled in Tahama, whereas severe-severity material was sampled in Koji. The recovered logs were numbered in the field and transported to the Iwate Prefectural Forestry Technology Center for subsequent processing and testing.

2.3 Mechanical evaluation of logs, small clear specimens, and laminae

The mechanical properties of fire-damaged Cryptomeria japonica logs, the laminae and small clear specimens obtained from them were evaluated according to the workflow shown in Fig. 2.

First, the dynamic longitudinal modulus of elasticity of the logs was measured by the longitudinal vibration method in accordance with the Japanese Agricultural Standard for logs, JAS 1052:2022. Log mass was measured using a crane scale (A&D FJ-T001), and the first-mode natural frequency of longitudinal vibration was measured using an FFT analyzer (Ono Sokki CF-4220Z). The apparent density of each log was calculated from the average end diameter, log length, and measured mass, and the dynamic longitudinal modulus was then calculated using the standard vibration equation specified in JAS.

For the evaluation of clear-wood mechanical properties, one butt log from each burn severity class was sawn by wood type, i.e., sapwood, mature heartwood, juvenile heartwood, and pith. The sawn materials were air-dried for 3 months to a moisture content of approximately 13–15%, and small clear specimens with dimensions of 20 mm × 20 mm × 500 mm were prepared. Static bending tests were then conducted in accordance with JIS Z 2101, and the modulus of rupture and modulus of elasticity were determined.

For lamina production, 19 logs from each burn severity class were sawn into laminae, kiln-dried to a moisture content of approximately 10%, and planed to final dimensions of approximately 108 mm × 28 mm × 2000 mm. In total, 711 laminae were prepared: 228 from the low-severity class, 254 from the moderate-severity class, and 229 from the severe-severity class. The laminae were machine graded using a mechanical grading machine (Iida Kogyo MGN101) in accordance with JAS 1152, the Japanese Agricultural Standard for glued laminated timber. Bending modulus classes were assigned from L30 to L125. Selected laminae sawn from the outermost wood zone immediately beneath the bark were further cut into specimens for tensile and C-type bending tests in accordance with JAS 1152. This sampling position was selected because the outermost wood was expected to have been most strongly affected by heat during burning.

For comparison, previously measured data from sound regional *C. japonica* were used as reference datasets. The log reference dataset consisted of 60 sound 4-m logs from the Kesen area, and the lamina reference dataset consisted of 748 kiln-dried laminae processed and graded under comparable industrial conditions. These reference data were used only for descriptive comparison and were not treated as a fully controlled experimental control group.

2.4 Bark condition

Disk samples with a thickness of 50 mm were collected from the log sections for bark-thickness measurement, microscopic observation, and chemical analysis, as shown in Fig. 2. Bark thickness was measured in four radial directions on each disk. Particular attention was given to the severe-severity class because field inspection indicated that charring was generally confined to the bark, whereas the remaining bark layer was markedly thinner and was easily detached during handling and debarking.

2.5 Microscopic observation, chemical composition, FT-IR, and WAXD/XRD analyses

For microscopic and chemical analyses, a representative severe-severity disk sample showing discoloration near the bark, disk No. 67, was selected. After removing approximately 5 mm from the outer surface, including the charred and visually affected surface layer, sapwood was sampled sequentially from the outside toward the pith on an annual-ring basis.

To determine the sugar content and Klason lignin, the wood powder sample (20 mg) were heated in 0.3 mL of 72 wt% H_2SO_4 at 30 ˚C for 60 min, with occasional shaking. The reaction solutions were diluted with 8.4 mL of ultra-pure water to 4 wt% H_2SO_4, and heated in an autoclave at 120 ˚C for 60 min. The supernatant was neutralized with barium carbonate until the pH reached neutral. The neutralized solution was centrifuged at 6,000 rpm for 5 min. The supernatant was filtered through a 0.22 μm PTFE syringe filter, and subjected to HPLC analysis. Analysis was performed with an HPLC system (JASCO, Tokyo, Japan) consisting of PU-4180 HPLC pump, AS-4050 HPLC autosampler, integrated with an SSC-2120 column oven (Senshu Scientific Co., Ltd., Tokyo, Japan) and a 1260 Infinity II evaporative light scattering detector (ELSD; Agilent Technologies, CA, USA). Samples (20 μL) were separated using an Aminex HPX-87P column (300 × 7.8 mm, Bio-Rad Laboratories, CA, USA) equipped with a Micro-Guard Carbo-P Refill Cartridge (30 × 4.6 mm, Bio-Rad Laboratories) at 85 ˚C. The mobile phase was ultrapure water, degassed via ultrasonication for 10 min, and delivered at a flow rate of 0.6 mL min^{-1}. Calibration curves were constructed using glucose, xylose, and mannose standards to determine the monosaccharide concentrations in the samples. The residues (Klason lignin) were washed with ultrapure water until a neutral pH was attained, and then freeze-dried. Finally, the corresponding ratios relative to the initial solids were calculated.

The Fourier-transform infrared (FT-IR) spectra of the wood powder were recorded using an FT-IR spectrometer (FT/IR-4700, JASCO, Tokyo, Japan) in the attenuated total reflection (ATR) mode in the 4000–500 cm^{-1} range at a resolution of 4 cm^{-1}, with 64 scans. Additional microscopic observation was conducted for moderate-severity material in which localized internal discoloration was observed.

Wide-angle X-ray diffraction (WAXD) measurements were performed using material cut from the same block used for the chemical analyses. Rod-like specimens were prepared from individual annual rings, starting from the bark side and proceeding inward. Each specimen was approximately 1 mm × 1 mm in cross section and approximately 1 cm in the fiber direction. Seven annual-ring positions were analyzed from the outer side toward the inner side; the third, relatively wide annual ring was divided into two specimens for measurement. WAXD measurements were conducted using a Rigaku RA-Micro7 HFMR equipped with a HyPix-6000HE detector and a Mo X-ray source operated at 50 kV and 24 mA. During measurement, the specimens were rotated to reduce anisotropy in the radial–tangential plane. Equatorial intensity profiles, corresponding to the direction perpendicular to the fiber axis, were obtained to evaluate whether the crystalline structure of cellulose was retained.

Thermogravimetric and differential thermal analyses were conducted under a nitrogen atmosphere using a DTG-60AH instrument. Approximately 2 mg of powdered wood sample was placed in an alumina cell, and nitrogen was supplied at a flow rate of 100 mL min^{-1}. The temperature program consisted of heating from 50 to 105°C at 30°C min^{-1}, holding at 105°C for 15 min to remove moisture, and subsequently heating to 900°C at 5°C min^{-1} under nitrogen. These analyses were used as supporting measurements to examine possible changes in the thermal degradation behavior of the burned wood.

2.6 Chlorine analysis for seawater-suppression risk

The samples were obtained as separate field sample sets. One sample set was collected from a burned area affected by aerial seawater spraying; a representative severe-severity sample in this area was collected from W1, where the observed height of stem charring was approximately 3.8–4.0 m. A second sample set was collected independently from another burned area (W2) where seawater was directly applied from the ground by firefighters during extinguishing operations. The directly extinguished samples were therefore not collected from the aerial-spraying area and are treated here as a separate sample group. Regional non-burned material was used as a background control for comparison. Sapwood samples were obtained by drilling four points in the sapwood zone, combining the chips, milling them, and sieving them to below 1 mm. Bark samples were collected from the outer side adjacent to the sapwood and treated in the same way. The milled sawdust was dried in an oven at 105°C for more than 24 h prior to use. Approximately 0.2 g of each sample was combusted in a tube furnace under synthetic air at 1 L min^{-1} and 800°C for 30 min. Chloride released during combustion was trapped in tandem alkaline absorption solutions, and washings from the combustion tube were recovered separately. The sum of the absorption solution and washings was interpreted as volatile chlorine. Residual ash was then extracted with hot water and analyzed as non-combustible chlorine. Chloride ion concentration in each fraction was quantified by ion chromatography. A schematic diagram of the apparatus used for the chlorine concentration measurement is provided in **Fig. S4**.

2.7 Data treatment and scope of interpretation

Parts of the mechanical grading and strength-related results were previously disseminated in Japanese as local administrative reports, newsletter or magazine articles (Forestry Promotion Division, Iwate Prefecture 2026; Nakayasu 2026; Yamaguchi 2025, 2026). For chemistry and microscopy, the present paper emphasizes what can be stated robustly from the available evidence and avoids over-interpreting exploratory observations from a limited number of representative samples.

3. Results

3.1 Dynamic modulus of logs

The dynamic longitudinal modulus of elasticity of the 60 logs is shown by burn-severity class in Fig. 3a. The distributions did not show a monotonic shift toward lower MOE classes with increasing burn severity at approximately three months after fire extinguishment. The modal class was Ef70 in all three burn-severity classes. Low- and severe-severity logs covered a similar range, from Ef50 to Ef110, whereas moderate-severity logs were distributed within a narrower range, from Ef50 to Ef90. Thus, the severe-severity class, despite having the most pronounced external charring, did not show a lower log stiffness distribution than the low- or moderate-severity classes.

The density-class distribution also did not indicate a systematic reduction associated with burn severity (Fig. 3b). Because the dynamic longitudinal modulus of logs is influenced by both density and longitudinal vibration characteristics, the absence of a clear downward shift in either parameter suggests that heat exposure had not caused substantial loss of whole-log stiffness in the remaining stem wood. The narrower distribution observed in the moderate-severity group is more likely to reflect ordinary tree-to-tree or site-related variation than a direct effect of fire, because the severe-severity group retained logs in the higher Ef classes.

These results indicate that visual stem blackening was not a reliable predictor of immediate whole-log stiffness loss in the present material. In other words, the field burn-severity classification captured the degree of bark charring and external exposure more clearly than it captured changes in longitudinal stiffness of the log. This distinction is important for post-fire salvage decisions: logs with severe external charring should not be rejected solely on the basis of visual appearance, but should instead be evaluated by standard mechanical grading. The subsequent lamina grading results provide a further test of whether this retained log-level stiffness was maintained after sawing, drying, and planing.

1. (a) Percentage distribution of longitudinal-vibration MOE classes determined according to Log JAS.
2. (b) Percentage distribution of log-density classes.

Each burn-severity class contained 20 logs. The reference group consisted of 60 sound 4-m *C. japonica* logs from the Kesen area.

3.2 Machine grading of laminae

Machine grading of the 711 kiln-dried laminae provided a direct assessment of whether wildfire-exposed logs retained grade-assessed stiffness after sawing, drying, and planing. As shown in Fig. 4, the grade distributions of laminae obtained from the low-, moderate-, and severe-severity classes broadly overlapped with those of the reference *C. japonica* laminae. In all three burn-severity classes, the majority of laminae were distributed within the structurally useful middle-grade range, particularly from L50 to L80. Importantly, the severe-severity group did not show an increased proportion of out-of-grade or low-grade laminae.

The grade ranges also did not indicate a deterioration trend with increasing burn severity. Low-severity laminae ranged from out-of-grade to L125, moderate-severity laminae from out-of-grade to L100, and severe-severity laminae from L30 to L110. The modal class was L60 in the low- and moderate-severity groups, whereas the severe-severity group showed a modal class of L70. The severe group also retained a substantial proportion of laminae in the L70–L90 range. Therefore, severe external charring did not translate into a downward shift in machine-graded lamina stiffness.

The slightly higher modal class observed in the severe-severity group should not be interpreted as a strengthening effect of fire. Because the severity classes were sampled from different trees and partly different stands, this difference is more plausibly attributed to ordinary stand-to-stand, tree-to-tree, and within-stem variation in *C. japonica* stiffness. Nevertheless, the absence of a low-grade shift in the severe group is important, because it indicates that the internal wood remaining after removal of visibly charred surfaces could still be processed into laminae with stiffness distributions comparable to those of sound regional material.

From a reuse perspective, these results provide evidence against blanket rejection of wildfire-exposed *C. japonica* based solely on external scorching. When the material was processed through normal industrial steps and graded mechanically according to JAS, most

laminae remained assignable to structural grade classes. In the associated utilization assessment, approximately 99% of all laminae could be incorporated into a symmetric mixed-grade glued-laminated timber layup equivalent to E55-F200, provided that machine grading rather than visual burn appearance was used as the primary selection criterion. Thus, the limiting factor for reuse is unlikely to be immediate loss of lamina stiffness alone; rather, it is more likely to involve bark degradation, debarking difficulty, cracking, storage duration, and logistics before processing.

Percentage occurrence of laminae obtained from the low, moderate, and severe classes, compared with reference laminae.

The number of laminae was n = 228 for the low class, n = 254 for the moderate class, n = 229 for the severe class, and n = 748 for the reference group.

3.3 Bending properties of small clear specimens

The static bending properties of the small clear specimens prepared in accordance with JIS Z 2101 are summarized in Fig. 5. The distributions of MOR and MOE differed depending on wood type, but they did not show a monotonic decrease with increasing burn severity. In the low-severity class (Fig. 5a,b), sapwood specimens were mainly distributed in relatively high MOR classes, whereas juvenile heartwood and pith-containing specimens tended to appear in lower MOR and MOE classes. The moderate-severity class showed broader distributions (Fig. 5c,d), with sapwood and mature heartwood mainly distributed around intermediate MOR and MOE classes, while juvenile heartwood and pith specimens were more frequently found in lower MOE classes.

Importantly, the severe-severity class did not exhibit a systematic reduction in bending properties (Fig. 5e,f). Sapwood and mature heartwood from severely burned logs were distributed mainly in relatively high MOR and MOE classes. In particular, the MOE distribution of severe-severity sapwood and mature heartwood was shifted toward higher classes compared with the juvenile heartwood and pith specimens. By contrast, juvenile heartwood and pith-containing specimens showed lower MOE values irrespective of burn severity. This indicates that the variation in bending properties was governed more strongly by radial wood type and the presence of juvenile or pith wood than by the external degree of burning.

These results suggest that severe external burning did not necessarily cause measurable deterioration of the remaining inner wood when sound small clear specimens were prepared after removing visibly charred portions. The lower stiffness observed in juvenile heartwood and pith specimens is consistent with the expected radial variation in wood quality, rather than with fire-induced degradation alone. Therefore, visual burn severity should not be used as the sole criterion for judging the mechanical usability of fire-damaged logs. Instead, mechanical grading and wood-type-based sorting are necessary to identify portions that retain sufficient strength and stiffness for material use.

Distributions of modulus of rupture (MOR) and modulus of elasticity (MOE) are shown for the low class (a, b), moderate class (c, d), and severe class (e, f).

Within each severity class, specimens from sapwood, mature heartwood, juvenile heartwood, and the pith region were compared. The vertical axis indicates percentage occurrence within each radial-position group.

3.4 External appearance and bark condition

Field observations in July 2025 indicated that, even in the severe-severity class, visible carbonization was generally concentrated in the bark and outer surface. Deep charcoal penetration into the xylem was not commonly observed at the time of harvest. However, bark condition differed markedly among burn-severity classes. The severe-severity logs often had a thin and easily detachable bark layer, whereas low- and moderate-severity material retained a more typical bark appearance.

The bark-thickness distribution confirmed this visual impression (Fig. 6). In the low- and moderate-severity classes, most measurements were distributed between 2 and 5 mm. By contrast, the severe-severity class was strongly concentrated in the thinner classes: approximately 60% of measurements were in the 1.00–1.99 mm class and approximately 14% were below 1 mm. Thus, approximately 75% of severe-severity measurements were below 2 mm, and values above 4 mm were almost absent.

These results show that the most conspicuous physical effect of severe burning was the loss of bark protection rather than deep carbonization of the xylem. Because reduced bark thickness can increase susceptibility to drying, checking, insect attack, and fungal colonization during post-fire storage, severe-severity logs may deteriorate rapidly if salvage and processing are delayed. Thus, the bark data complement the mechanical grading results: although short-term stiffness was retained, the severe-severity material likely had a higher risk of time-dependent degradation.

3.5 Microscopic observations and chemical/crystallographic integrity of internal wood

A representative severe-severity disk, disk No. 67, was selected for microscopic and chemical examination because slight discoloration was observed near the bark-facing xylem. Macroscopic observation showed severe external damage at the bark surface, but no obvious deep penetration of charcoal into the xylem. In transverse microscopic sections, the cell-wall framework of the tracheids was clearly retained both in the severe-severity sample and in the non-burned control (Fig. 7). Brown-colored deposits were locally observed in the lumina of latewood tracheids in the severe-severity sample. These deposits were more consistent with resinous or extractive substances than with collapse or disappearance of the cell-wall structure. The outermost xylem consisted mainly of latewood, and no newly formed earlywood was observed outside this zone, suggesting that cambial activity had ceased after the fire, probably as a result of lethal heating of the cambial region.

The upper row shows the severe-severity sample, disk No. 67, and the lower row shows the non-burned control. The left column shows disk cross sections and sampling locations, the middle column shows small specimens excised from the indicated regions, and the right column shows transverse microscopic sections. White rectangles indicate the regions selected for microscopic observation.

Annual-ring samples were prepared sequentially from the bark side toward the pith using a radial strip cut from the severe-severity disk, as shown in Fig. 8a. The numbers and colors of the spectra and diffraction profiles correspond to the radial positions indicated in the specimen image. This sampling scheme was used to examine whether chemical or crystallographic changes were concentrated near the bark-facing xylem or progressed inward along the radial direction.

FT-IR spectra normalized near 1030 cm^{-1} showed similar relative intensities of carbohydrate-related bands at approximately 895, 1160, and 1730 cm^{-1} and lignin-related bands at approximately 1265 and 1510 cm^{-1} between the severe-severity annual-ring samples and the non-burned control (Fig. 8b). In particular, the carbonyl band near 1730 cm^{-1}, which is commonly associated with acetyl and carboxyl groups in hemicellulose, did not show a clear decrease relative to the control. Likewise, the lignin aromatic skeletal band near 1510 cm^{-1} was retained. These results indicate that the principal FT-IR markers of hemicellulose, cellulose, and lignin were preserved in the analyzed internal wood.

WAXD/XRD profiles further showed that cellulose crystalline structure was retained across the annual-ring positions. Reflections assigned to cellulose Iβ, including the (1–10), (110), and (200) planes, were observed from the bark-adjacent position to the inner positions (Fig. 8c). No systematic change in peak width was detected from the outer side toward the inner side. Thus, the analyzed wood did not show evidence of progressive loss or disordering of cellulose crystallites along the radial direction.

(a) Annual-ring sampling positions in a radial strip prepared from the bark side toward the pith. The numbers and colors correspond to the FT-IR spectra and WAXD/XRD profiles shown in panels b and c. (b) FT-IR spectra used to evaluate the retention of characteristic functional groups of hemicellulose, cellulose, and lignin. (c) WAXD/XRD profiles used to evaluate the retention of cellulose Iβ crystalline structure.

The ring-by-ring chemical composition of the same severe-severity sample is summarized in Table 1. The samples taken from the 1st, 2nd, 4th, and 9th annual rings from the outer surface contained 41–46% glucose, 4–5% xylose, 6–7% mannose, and 37–41% lignin, with total values of 93–99%. These values were broadly comparable to those of the non-burned control wood collected from the same region, which contained 44–46% glucose, 5% xylose, 6–8% mannose, and 35–37% lignin. No monotonic decrease in glucose, xylose, or mannose was observed from the outer annual rings toward the inner annual rings. Although lignin content in the severe-severity sample was slightly higher than that of the control in some positions, this difference was not accompanied by a systematic decrease in carbohydrate components. Therefore, within the resolution of the present dataset, severe external burning did not produce a marked alteration in the bulk carbohydrate or lignin composition of the remaining internal wood. The detailed compositional data are summarized in **Table S1** as descriptive statistics, and these differences should be interpreted cautiously because the dataset was limited and was not designed for replicate-based statistical testing.

Table 1
Chemical composition by annual-ring position

Fire-damage class	Ring position from outside (yr)	Glucose (%)	Xylose (%)	Galactose (%)	Arabinose (%)	Mannose (%)	Lignin (%)	Total (%)
Severely burned	1	42	4	0	1	6	41	95
Severely burned	2	46	5	0	1	6	37	95
Severely burned	4	41	5	0	1	7	39	93
Severely burned	9	46	4	1	1	7	41	99
Control	1	44	5	0	1	8	35	94
Control	9	46	5	0	1	6	37	95

Note: Ring position is expressed as the number of annual rings counted from the outer surface of the wood piece. The control samples were non-burned wood collected from the same region. "Total" is the value provided in the original dataset and may not equal the simple arithmetic sum because of rounding and analytical convention.

TG analysis was also conducted on samples taken from the outermost ten annual rings. The resulting TG profiles were broadly comparable to those of the control sample, with no marked change in thermal weight-loss behavior (**Fig. S5**). These TGA results provide supporting evidence that the thermal degradation behavior of the analyzed internal wood was not markedly altered.

Overall, the microscopic observations, FT-IR spectra, WAXD/XRD profiles, chemical composition, and TGA results were mutually consistent. Although localized discoloration and lumen deposits were observed near the bark-facing xylem, the tracheid cell-wall framework, characteristic FT-IR bands, cellulose Iβ diffraction peaks, bulk lignocellulosic composition, and thermal weight-loss behavior were retained. Therefore, marked degradation of the internal wood was not detected even in the representative severe-severity sample.

This interpretation is consistent with the known thermal response of wood. Previous studies have shown that thermal modification or thermal loading changes wood chemistry primarily when sufficient temperature and exposure time are reached. Hemicelluloses are generally the most heat-sensitive cell-wall components, and their degradation is typically reflected by decreases in pentose-derived sugars and by changes in IR bands such as the carbonyl band near 1730–1736 cm^{-1} and the cellulose/hemicellulose band near 895–900 cm^{-1} (Chien et al. 2018; Dúbravská et al. 2024; Esteves and Pereira 2009; Hill et al. 2021). More severe heat treatment, particularly at high temperature and in the presence of oxygen, can induce hemicellulose deacetylation, lignin condensation or cross-linking, cellulose depolymerization, and changes in cellulose structure (Candelier et al. 2016; Chien et al. 2018; Hill et al. 2021).

In fire-exposed wood, however, the outer charred layer can act as a thermal barrier. Thermally loaded wood can develop a stratified structure from the exposed surface toward the interior, including charred, pyrolyzed, and relatively intact zones, which helps explain why severe external burning does not necessarily imply extensive degradation of internal xylem (Dúbravská et al. 2024; White and Dietenberger 2001). This framework explains why a specimen can appear severely burned on the exterior while the internal annual rings remain chemically and structurally close to non-burned wood. In the present samples, the lack of depletion in glucose, xylose, mannose, and hemicellulose-related IR bands, together with retention of cellulose Iβ diffraction peaks and comparable TG profiles, suggests that the analyzed internal wood did not experience a thermal history sufficient to cause extensive lignocellulosic degradation.

Accordingly, the most conservative interpretation is that marked degradation was not detected in the analyzed annual-ring samples. The small increase in lignin content observed in the severe-severity sample should be interpreted cautiously because it was not associated with a clear decrease in carbohydrate markers or a monotonic annual-ring trend. It may reflect natural within-tree variation, analytical variability, or relative rather than absolute enrichment. Thus, even in the severely burned wood, the FT-IR spectra, WAXD/XRD profiles, chemical composition, and TG behavior of the remaining annual-ring samples were close to those of the non-burned control.

3.6 Chlorine survey

A targeted chlorine survey was conducted to evaluate whether seawater-based fire suppression resulted in a measurable residual chlorine signal in burned *C. japonica*. In the analytical procedure used in this study, chlorine released during tube-furnace combustion

was quantified as chloride ion in alkaline absorption and tube-rinse solutions and was reported as volatile chlorine. Chloride extracted by hot water from the post-combustion ash was reported as non-combustible chlorine. The sum of these two fractions is used here as a calculated total chlorine equivalent. This value should be interpreted as a practical reference sum for comparing sample groups, not as a certified total-chlorine value obtained by a single standardized total-chlorine method.

The calculated total chlorine equivalent in the regional non-burned control material was 0.0284–0.0369% in bark and 0.0078–0.0117% in the sieved fraction. In the burned samples from the aerial seawater-spraying area, the corresponding values were 0.0043–0.0101% in bark and 0.0003–0.0042% in the sieved fraction. Many values in this sample set, particularly in the sieved fraction and in the non-combustible chlorine fraction, were below the quantification limit or below the detection limit.

In the separately collected samples from the area directly extinguished with seawater by firefighters, several volatile chlorine values were quantifiable. However, the calculated total chlorine equivalent remained 0.0042–0.0182% in sapwood and 0.0121–0.0173% in bark. These values did not exceed the range observed in the bark of the regional non-burned control material, although some values were higher than those observed in the control sieved fraction. Thus, within the limits of the present sample sets, neither the aerial seawater-sprayed samples nor the separately collected directly extinguished samples showed an unusually high chlorine concentration relative to the regional background bark values.

Chlorine is an important quality parameter for woody biomass fuel because chloride species and alkali chlorides, including KCl and NaCl, can contribute to HCl formation, ash deposition, fouling, and corrosion in biomass combustion systems (Dula and Kraszkiewicz 2025; Jafarihonar et al. 2025). As an indicative fuel-quality benchmark, ISO 17225-4 provides specifications and classes for graded wood chips (International Organization for Standardization 2021). In publicly available wood-fuel quality guidance based on the ISO 17225 series, the B1 and B2 classes for wood chips include a chlorine criterion of Cl 0.05% on a dry-mass basis (Alakangas 2020). The maximum calculated total chlorine equivalent observed in this study was approximately 0.0369% when the non-burned control bark was included and approximately 0.0182% in the separately collected directly seawater-extinguished burned samples. These values are below the 0.05% dry-mass reference level; however, the comparison should be regarded as indicative because the analytical values must be confirmed as dry-mass values or converted to a dry-mass basis before strict comparison with fuel specifications.

Overall, the present results do not support a clear residual salt-enrichment signal in the tested burned *C. japonica*. The relatively higher chlorine concentrations observed in the non-burned control bark suggest that regional background, bark-associated deposits, and material fraction can strongly influence chlorine concentrations. Therefore, the present data do not justify rejecting the tested burned *C. japonica* as biomass fuel solely on the basis of chlorine concentration. However, practical fuel acceptance should be based on lot-scale quality control and should include moisture content, ash content, alkali metals such as Na and K, sulfur, calcium, silicon, ash melting behaviour, fuel blending ratio, and actual boiler operating conditions. Additional sampling across burned stands, suppression methods, and collection areas would be required before generalizing this conclusion to all seawater-suppressed burned wood.

Table 2
Summary of chlorine concentrations in *C. japonica* samples exposed to seawater during firefighting operations

Exposure condition	Material fraction	n	Volatile Cl (%)	Non-combustible Cl (%)	Calculated total Cl (%)□
Non-burned control from the same area	Bark	2	0.0282–0.0367	0.00020	0.0284–0.0369
Non-burned control from the same area	Sieved fraction	2	0.0076–0.0115	0.00020	0.0078–0.0117
Aerial seawater spraying	Bark	3	0.0040–0.0098	0.00020–0.00030	0.0043–0.0101
Aerial seawater spraying	Sieved fraction	3	N.D.–0.0040	0.00020–0.00030	0.0003–0.0042□
Direct seawater extinguishing by firefighters on site	Sapwood	4	0.0041–0.0180	0.00013–0.00032	0.0042–0.0182
Direct seawater extinguishing by firefighters on site	Bark	4	0.0120–0.0170	0.000083–0.00028	0.0121–0.0173

□ Calculated total Cl is the sample-wise reference sum of volatile Cl and non-combustible Cl. It is not a certified total-chlorine value obtained by a single total-chlorine method.

 N.D. indicates below the detection limit. Values below the quantification limit were retained when calculating the concentration range. For reference summation only, N.D. values were treated as zero; totals involving N.D. should therefore be interpreted as lower-bound estimates.

4. Discussion

4.1 Mechanical retention despite severe external charring

The key finding of this study is that external burn severity was not directly associated with short-term loss of log or lamina stiffness. The burn-severity classes primarily reflected the degree of bark charring and external exposure, whereas the dynamic modulus of logs and the machine-graded bending modulus of laminae showed no monotonic decrease with increasing burn severity. The modal log class was identical among the three severity classes, and the lamina grade distributions broadly overlapped with those of sound regional *C. japonica*. In addition, the JIS Z 2101 bending tests of small clear specimens showed that the variation in MOR and MOE was governed more strongly by radial wood type than by visual burn severity.

This distinction is important for post-fire salvage decisions. In the field, blackened bark and surface charring can easily be interpreted as evidence of deep material damage. However, the present results indicate that visual burn severity alone was a poor predictor of immediate mechanical performance in the remaining wood. When wildfire-exposed C. japonica was harvested within approximately three months after extinguishment and processed through standard grading procedures, a large proportion of the material retained stiffness classes suitable for structural timber feedstock.

This interpretation is consistent with previous reports on post-fire conifers, where moderate fire exposure caused limited changes in density or stiffness, whereas more pronounced mechanical deterioration was associated with longer exposure, greater heat penetration, or more severe heating (Bortoletto Júnior and Moreschi 2003; Marttila et al. 2024). In the Ofunato material, heat penetration into the xylem was probably limited because much of the visible damage was concentrated in the bark and outermost surface. Thus, severe external charring did not necessarily imply degradation of the load-bearing wood substance.

4.2 Bark loss as the main post-fire deterioration risk

Although short-term stiffness was largely retained, bark degradation was pronounced in the severe-severity class. Approximately 75% of bark-thickness measurements in this class were below 2 mm, and the bark was often thin, brittle, or easily detached. This indicates that the major physical effect of severe burning was not deep carbonization of the xylem, but loss of the protective bark layer.

This finding has practical importance because bark protects stems against rapid moisture loss, surface checking, insect entry, and fungal colonization. Once this protection is lost, the material may deteriorate rapidly during standing, storage, transportation, and preprocessing. Therefore, the severe-severity logs should be regarded as mechanically promising but operationally fragile. The positive stiffness results should not be interpreted as evidence that the material can be left standing or stored for long periods without quality loss.

The results therefore suggest that the main risk for severely burned C. japonica is time-dependent deterioration rather than immediate stiffness loss. Prompt harvesting, debarking, drying, and grading are likely to be more important for severely burned logs than for low- or moderate-severity logs. This interpretation reconciles the apparently favorable mechanical grading results with the strong cautionary signals from bark thinning and bark detachment.

4.3 Chemical and crystallographic integrity of the internal wood

The microscopy, chemical composition, FT-IR, and WAXD/XRD results support the mechanical interpretation. In the representative severe-severity sample, localized discoloration and brown deposits were observed near the bark-facing xylem, but the tracheid cell-wall framework was retained. These deposits may reflect resinous or extractive redistribution, or a local wound-related response, rather than collapse or disappearance of the cell-wall structure. The absence of newly formed xylem outside the outermost latewood zone is consistent with cessation of cambial activity after the fire, probably due to lethal heating of the cambial region; however, this should be interpreted cautiously because cambial viability was not directly tested.

The ring-by-ring chemical composition showed no monotonic decrease in glucose, xylose, mannose, or total carbohydrate components from the outer annual rings toward the inner annual rings. FT-IR spectra retained the main carbohydrate-related bands near 895, 1160, and 1730 cm^{-1}, as well as lignin-related bands near 1265 and 1510 cm^{-1}. WAXD/XRD profiles also retained cellulose Iβ reflections,

including the (1–10), (110), and (200) planes, without a systematic outer-to-inner change in peak width. Taken together, these results indicate that marked degradation of the analyzed internal wood was not detected.

This interpretation is consistent with the known thermal response of wood. Hemicelluloses are generally the most heat-sensitive cell-wall components, and their degradation is often reflected by decreases in pentose-derived sugars and changes in FT-IR bands near 1730–1736 cm^{-1} and 895–900 cm^{-1}. More severe thermal treatment can also induce lignin condensation, cellulose depolymerization, and changes in cellulose crystallinity (Candelier et al. 2016; Chien et al. 2018; Esteves and Pereira 2009; Hill et al. 2021; White and Dietenberger 2001).

This does not mean that all fire-exposed wood was completely unaffected. Localized discoloration, extractive movement, molecular-weight changes, or subtle changes in thermal behavior may occur without producing large changes in bulk chemical composition or FT-IR spectra. Therefore, the most conservative conclusion is not that the wood was entirely unchanged, but that marked degradation was not detected in the analyzed internal annual-ring samples.

4.4 Chloride contamination and seawater suppression

The chlorine survey provides an additional practical perspective because seawater was used during firefighting operations. The measured chlorine concentrations did not indicate abnormal salt accumulation in the tested burned wood. In particular, the calculated total chlorine values for samples directly extinguished with seawater were lower than those observed in the non-burned control bark collected from the same region. This suggests that, within the scope of the present sampling, seawater-based suppression did not leave a strong residual chloride signal in the analyzed sapwood or bark.

This result is relevant because seawater-derived chloride contamination could otherwise become an additional reason to reject fire-suppressed wood for material or fuel use. However, the present chlorine dataset should be interpreted as a representative survey rather than a comprehensive spatial assessment. Chloride deposition may vary with firefighting method, seawater exposure, rainfall after the fire, bark condition, surface roughness, and sampling position. Therefore, broader sampling would be required before generalizing the result to all burned stands or all suppression conditions. Nevertheless, the available data do not support blanket exclusion of the tested material on the basis of chloride contamination.

4.5 Practical implications and limitations

As discussed above, the bark of the damaged trees differed in its debarking behavior. In the severe class, bark sometimes peeled readily by hand, whereas lower-severity material could reportedly be more difficult to debark using water-pressure barkers. Carbonized bark and concern about blade damage to debarking blades may lead operators to adopt water-assisted or otherwise modified debarking procedures, increasing labor and cost even before formal grading begins.

Economic and institutional constraints may also limit rapid salvage utilization. Japanese forestry is structurally constrained by low timber revenues, high harvesting and silvicultural costs, and strong dependence on subsidies and forest owners' associations (Fuchigami et al. 2016; Takahashi et al. 2021). Previous research on Japanese forest management has shown that income distributed through ordinary forest management and timber distribution processes can be too low to allow forest owners to conduct sufficient silviculture, while rural depopulation, aging forest owners, and absentee ownership further weaken owners' direct engagement in forest management (Fuchigami et al. 2016). This point is also consistent with the Otsuchi–Kesen River Regional Forest Plan, which attributes the low implementation rate of artificial reforestation partly to declining management motivation among forest owners (Iwate Prefecture 2024). In the Ofunato case, public support may cover felling and reforestation costs; however, if forest insurance and log transportation costs remain burdens for owners, such residual costs may slow consent formation and implementation even when rapid removal of burned trees is technically desirable.

A second constraint concerns the capacity of the regional forestry and wood-processing system. The Otsuchi–Kesen River Regional Forest Plan reports that the planning area had approximately 180,000 m^3 of annual roundwood production in 2022, including 173,000 m^3 of coniferous roundwood (Iwate Prefecture 2024), and the burnt volume is estimated to be much larger than this; Of the 3,370 ha of damaged forest reported in the official damage survey, 1,785 ha was classified as planted forest (Ofunato City 2025). Assuming an average standing volume of approximately 310–390 m^3/ha for these planted forests, the resulting standing timber volume in the wildfire-damaged planted forests would be roughly 560,000–700,000 m^3. This corresponds to approximately three to four times the annual roundwood production of the planning area. Such a sudden volume shock would require extraordinary coordination among logging contractors, haulers, temporary log yards, log markets, processors, biomass users, and administrative bodies. Therefore, even if

wildfire-damaged *C. japonica* is physically suitable for reuse, actual utilization may be constrained by the capacity of salvage logistics and downstream demand.

This paper has several limitations. First, it represents a single wildfire case in a single dominant species, and the results may not transfer directly to other fire regimes, storage durations, or species. Second, the chemical interpretation is still based on a limited number of representative discolored samples, and the chlorine survey was intentionally conservative in scope.

Future work should therefore address at least three issues: (i) small-specimen testing and thermal analysis to clarify whether subtle heat effects occurred without obvious spectral changes; (ii) time-dependent monitoring of bark loss, cracking, biodeterioration, and residual value in standing and stored logs; and (iii) integrated economic evaluation of salvage, transport, debarking, grading, and downstream product use.

5. Conclusions

This study evaluated the reuse potential of wildfire-exposed Cryptomeria japonica recovered approximately three months after extinguishment of the 2025 Ofunato wildfire. The following conclusions were obtained:

1. Dynamic log modulus and machine-graded lamina bending modulus showed no monotonic decrease with increasing visual burn severity. The modal log class was identical among severity classes, and the lamina grade distributions were broadly comparable to those of sound regional *C. japonica*.
2. JIS Z 2101 bending tests of small clear specimens indicated that MOR and MOE were influenced more strongly by radial wood type than by external burn severity. Sapwood and mature heartwood from severely burned logs retained relatively high bending properties, whereas juvenile heartwood and pith-containing specimens tended to show lower stiffness irrespective of burn severity.
3. Severe external burning was associated primarily with bark thinning and bark detachment. Approximately 75% of bark-thickness measurements in the severe-severity class were below 2 mm, indicating loss of the protective bark layer and increased risk of time-dependent deterioration during standing, storage, and processing.
4. Microscopy, chemical composition, FT-IR spectra, and WAXD/XRD profiles provided no clear evidence of marked degradation in the analyzed internal wood. The principal carbohydrate and lignin components, characteristic FT-IR bands, and cellulose Iβ diffraction peaks were retained in the representative severe-severity sample.
5. Chlorine measurements did not indicate abnormal salt accumulation in the tested burned wood relative to non-burned control material from the same region, although broader sampling is needed to evaluate spatial variation in seawater-suppression effects.

Overall, promptly salvaged wildfire-exposed *C. japonica* should not be rejected solely on the basis of visual charring. The results support a grading-based decision framework for allocating fire-exposed logs to engineered-wood feedstock, while emphasizing that rapid harvest, debarking, drying, mechanical grading, and further verification of destructive strength, bonding performance, durability, and storage effects are necessary before final product-level use.

Declarations

Competing interests

The authors declare that they have no competing interests.

Ethics approval

Not applicable.

Author Contribution

Y.N. conceived and designed the study, participated in tree felling, developed the sampling strategy, performed wood milling, thermogravimetric analysis, and total chlorine measurements, assisted with mechanical property measurements, acquired funding, and wrote the original draft. K.Y. performed the mechanical property evaluations and prepared the workflow diagram. K.K. performed the

microscopic observations and X-ray diffraction analyses. Y.N. contributed to chemical analysis, FT-IR measurement and discussion of the analytical results. K.R. contributed to wood milling, sample preparation, thermogravimetric analysis, and assistance with mechanical property measurements. K.M. contributed forestry expertise and discussed the economic and operational constraints of post-fire salvage and utilization. T.T. provided overall advice during manuscript revision. H.T. supervised the mechanical property evaluations, performed bark-thickness measurements, and provided technical advice throughout the study. Y.T. designed the study and provided information on the Ofunato wildfire, acquired funding, selected field sites, coordinated procedures related to tree felling, and supervised the overall study. All authors reviewed and approved the final manuscript.

Acknowledgement

This work was supported by the Japan Society for the Promotion of Science (JSPS) KAKENHI Grant Numbers 25K21634 and 24H00336. The authors are deeply grateful to E on Hirabayashi and Takashi Miyakawa for their assistance with the felling of *C. japonica*. The authors also gratefully acknowledge the collaborative research conducted between Kyoto University and Tohoku University as part of a broader collaborative research framework involving Daicel Corporation. The authors further acknowledge the generous support provided by FRIS CoRE, Tohoku University, a shared research facility.

Data availability

The datasets generated and analyzed during the current study are available from the corresponding author upon reasonable request.

References

1. Alakangas E (2020) Quality guidelines for wood fuels in Finland—2020. VTT-M-04712-15. Bioenergy Association of Finland, Finnish Energy, Finnish Forest Industries Federation, Helsinki
2. Barčić D, Antonović A, Rosavec R, Dubravac T, Ančić M, Ištvanić J (2022) The chemical composition changes of Aleppo pine (Pinus halepensis Mill.) and black pine (Pinus nigra J.F. Arnold) wood after a forest fire: usability for bioproducts. Environ Sci Proc 17:39. https://doi.org/10.3390/environsciproc2022017039
3. Bortoletto Júnior G, Moreschi JC (2003) Physical-mechanical properties and chemical composition of Pinus taeda mature wood following a forest fire. Bioresour Technol 87:231–238. https://doi.org/10.1016/S0960-8524(02)00242-0
4. Candelier K, Thevenon MF, Petrissans A, Dumarcay S, Gerardin P, Petrissans M (2016) Control of wood thermal treatment and its effects on decay resistance: a review. Ann Sci 73:571–583. https://doi.org/10.1007/s13595-016-0541-x
5. Chien YC, Yang TC, Hung KC, Li CC, Xu JW, Wu JH (2018) Effects of heat treatment on the chemical compositions and thermal decomposition kinetics of Japanese cedar and beech wood. Polym Degrad Stab 158:220–227. https://doi.org/10.1016/j.polymdegradstab.2018.11.003
6. Dúbravská K, Kučerová V, Štefková J, Mišíková O (2024) Charring of and chemical changes in historical wood under thermal loading. Forests 15:1189. https://doi.org/10.3390/f15071189
7. Dula M, Kraszkiewicz A (2025) A review: problems related to ash deposition and deposit formation in low-power biomass-burning heating devices. Front Energy Res 13:1652415. https://doi.org/10.3389/fenrg.2025.1652415
8. Esteves BM, Pereira HM (2009) Wood modification by heat treatment: a review. BioResources 4:370–404. https://doi.org/10.15376/biores.4.1.370-404
9. Fire and Disaster Management Agency (2025) Report by the Commissioner of the Fire and Disaster Management Agency on the fire-cause investigation of the wildfire in Ofunato City that occurred on 26 February 2025. Fire and Disaster Management Agency, Tokyo. https://www.fdma.go.jp/singi_kento/kento/post-167.html. Accessed 16 June 2026. In Japanese
10. Forest Management Center (2024) Reforestation and restoration of a wildfire site through the Water Source Forest Development Project: Ozaki–Shirahama afforestation site, Kamaishi, Iwate Prefecture. Suigenrin 12:2–5 In Japanese
11. Forestry Agency (2025) Annual report on forest and forestry in Japan: fiscal year 2024 (summary). Ministry of Agriculture, Forestry and Fisheries, Japan, Tokyo. https://www.maff.go.jp/e/data/publish/AnnualReportonForestandForestry/AnnualReportonForestandForestryinJapan_FY2024.pdf. Accessed 16 June 2026

12. Division FP, Iwate Prefecture (2026) Development of construction-type emergency temporary housing using Iwate-grown timber after the Ofunato forest fire and initiatives toward use of fire-damaged timber. Jutaku Mokuzai 49(559):30–31 In Japanese
13. Fuchigami Y, Hara K, Uwasu M, Kurimoto S (2016) Analysis of the mechanism hindering sustainable forestry operations: a case study of Japanese forest management. Forests 7:182. https://doi.org/10.3390/f7080182
14. Hill CAS, Altgen M, Rautkari L (2021) Thermal modification of wood—a review: chemical changes and hygroscopicity. J Mater Sci 56:6581–6614. https://doi.org/10.1007/s10853-020-05722-z
15. International Organization for Standardization (2021) ISO 17225-4:2021, Solid biofuels—fuel specifications and classes—Part 4: Graded wood chips. International Organization for Standardization, Geneva
16. Iwate P (2024) Otsuchi–Kesen River Regional Forest Plan, Otsuchi–Kesen River Forest Planning Area: established in FY2024, planning period 1 April 2025–31 March 2035. Iwate Prefecture, Morioka. https://www.pref.iwate.jp/sangyoukoyou/ringyou/seibi/1008333/1008334.html. Accessed 16 June 2026. In Japanese
17. Jafarihonar F, Vainio E, Hupa L, Hupa M (2025) Low-temperature corrosion in large-scale biomass boilers. npj Mater Degrad 9:108. https://doi.org/10.1038/s41529-025-00640-4
18. Korkut S, Akgül M, Dündar T (2008) The effects of heat treatment on some technological properties of Scots pine (Pinus sylvestris L.) wood. Bioresour Technol 99:1861–1868. https://doi.org/10.1016/j.biortech.2007.03.038
19. Marttila J, Möttönen V, Haapala A, Ylimäki P, Kilpeläinen P, Verkasalo E (2024) Wood material properties of forest fire-damaged Norway spruce and Scots pine for mechanical wood processing in Finland. Appl Sci 14:238. https://doi.org/10.3390/app14010238
20. Nakayasu Y (2026) Utilization potential of fire-damaged timber from the Ofunato forest fire and its regional implications. Mokuzai Joho 417:1–6 In Japanese
21. Ofunato City (2025) Forest area damaged and estimated monetary damage associated with the 2025 large-scale forest fire in Ofunato City. Ofunato City press release, 28 October 2025. https://www.city.ofunato.iwate.jp/archive/p20251028104404. Accessed 16 June 2026. In Japanese
22. Sasa T, Hasegawa K, Goto K (1989) Case analysis for establishing a method to predict post-fire tree survival from the degree of stem scorching by surface fire: health condition of mature sugi trees two years after fire damage. Shinrin Richi 31(2):46–54. https://doi.org/10.18922/jjfe.31.2_46In Japanese
23. Takahashi T, de Jong W, Kakizawa H, Kawase M, Matsushita K, Sato N, Takayanagi A (2021) New frontiers in Japanese forest policy: addressing ecosystem disservices in the 21st century. Ambio 50:2272–2285. https://doi.org/10.1007/s13280-021-01566-2
24. Touge Y, Shi K, Nishino T, Sun C, Sekizawa A (2024) Spatial-temporal characteristics of more than 50,000 wildfires in Japan from 1995 to 2020. Fire Saf J 142:104025. https://doi.org/10.1016/j.firesaf.2023.104025
25. White RH, Dietenberger MA (2001) Wood products: thermal degradation and fire. In: Buschow KHJ, Cahn RW, Flemings MC, Ilschner B, Kramer EJ, Mahajan S, Veyssière P (eds) Encyclopedia of materials: science and technology, 2nd edn. Elsevier, Amsterdam, pp 9712–9716. https://doi.org/10.1016/B0-08-043152-6/01763-0
26. Yamaguchi K (2025) Evaluation of physical and mechanical properties of fire-damaged timber from the Ofunato forest fire. Iwate no Ringyo 816:4–5 In Japanese
27. Yamaguchi K (2026) Strength performance of fire-damaged timber from the Ofunato forest fire. Magariya 76:17–19 In Japanese
28. Yamaguchi K, Taniuchi H, Nakayasu Y, Kobayashi K, Touge Y (2026) Strength of fire-damaged sugi (Cryptomeria japonica) timber. In: Proceedings of the 76th Annual Meeting of the Japan Wood Research Society, poster D17-P1-07. In Japanese
29. Zachar M, Párničanová A, Kačíková D, Čabalová I, Zacharová L (2025) The effect of heat flux on the fire and chemical properties of oak wood (Quercus petraea). BioResources 20:860–876. https://doi.org/10.15376/biores.20.1.860-876

Figures

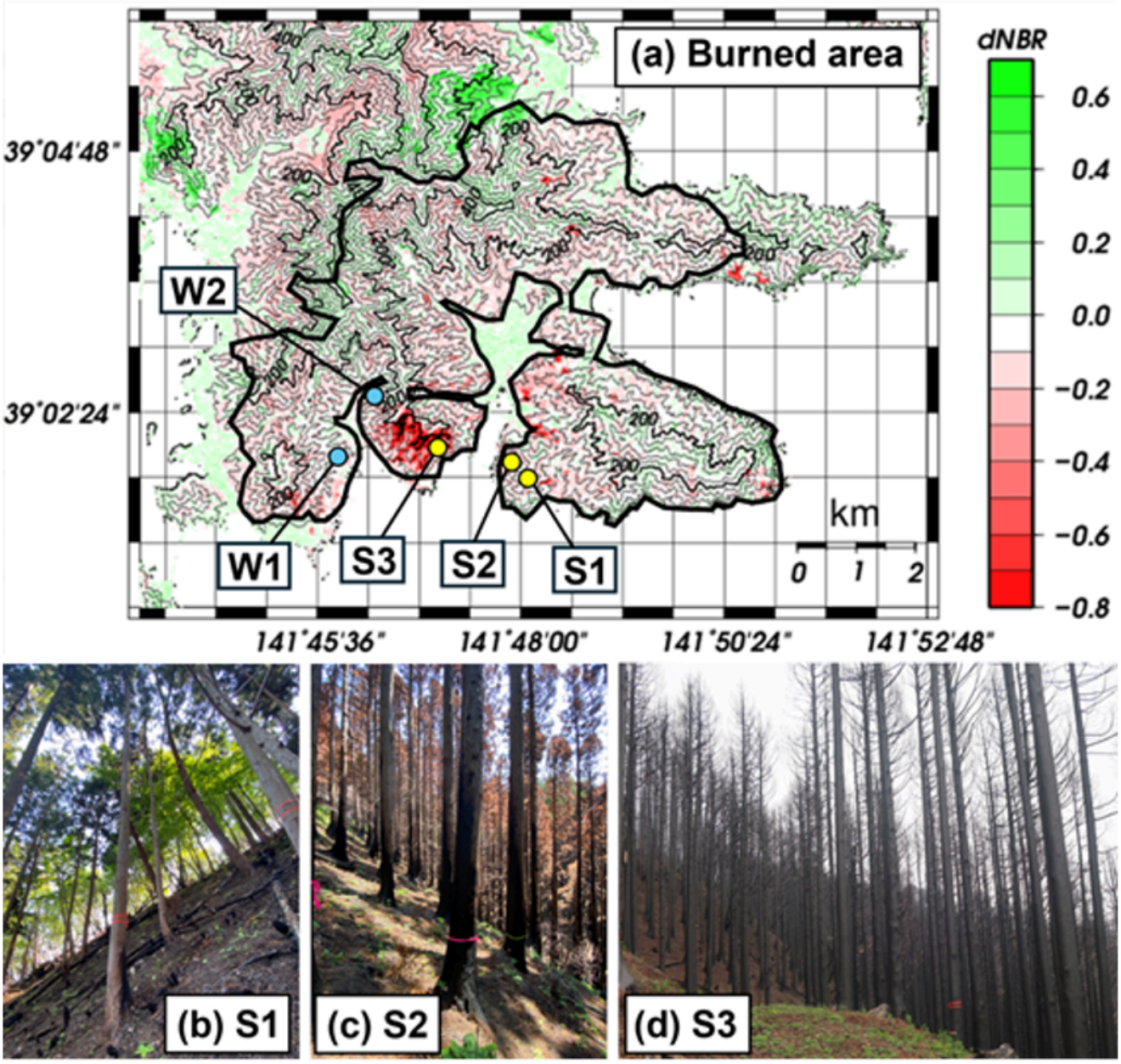


Figure 1

Study area and observed sites. S1–S3 indicate tree sampling sites under different fire severities. W1 and W2 are sampling sites for chlorine analysis; aerial firefighting was performed at W1, whereas ground-based firefighting was performed at W2. (a) Burned area of the 2025 Ofunato wildfire with satellite-derived burn severity shown in color. Burn severity was evaluated using the difference in the Normalized Burn Ratio (dNBR) observed by Sentinel-2, calculated as the difference between March 24, 2025 and March 12, 2024. The boundary of the burned area was based on data provided by the Fire and Disaster Management Agency. (b) Site S1 with low burn severity (May 29, 2025). (c) Site S2 with moderate burn severity (May 29, 2025). (d) Site S3 with severe burn severity (June 3, 2025).

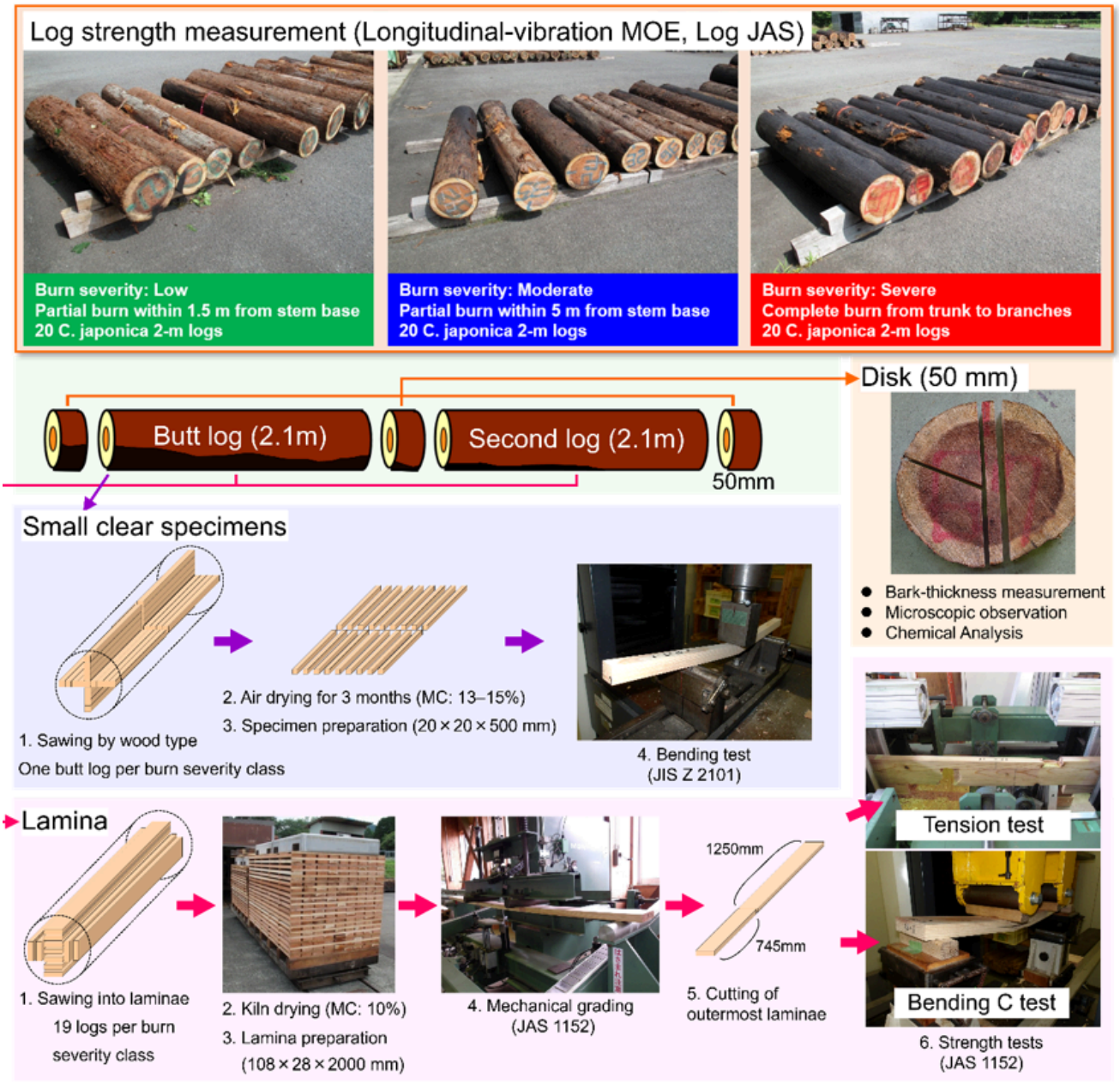


Figure 2

Sampling scheme and burn severity classes of fire-damaged Cryptomeria japonica logs used in this study. The upper diagram shows the positions of 5-cm disks and 2.1-m logs cut from each stem, and the lower photographs show representative logs classified as low, moderate, and severe burn severity.

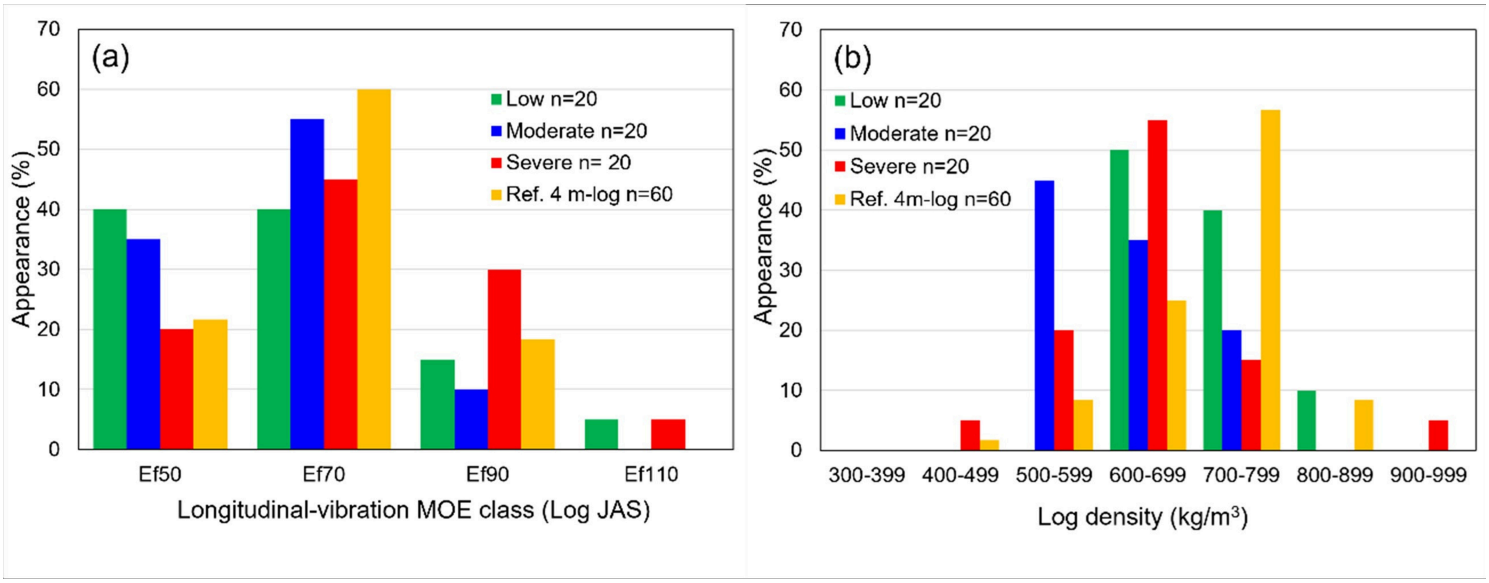


Figure 3

Distribution of log quality classes by burn severity.

(a) Percentage distribution of longitudinal-vibration MOE classes determined according to Log JAS.

(b) Percentage distribution of log-density classes.

Each burn-severity class contained 20 logs. The reference group consisted of 60 sound 4-m *C. japonica* logs from the Kesen area.

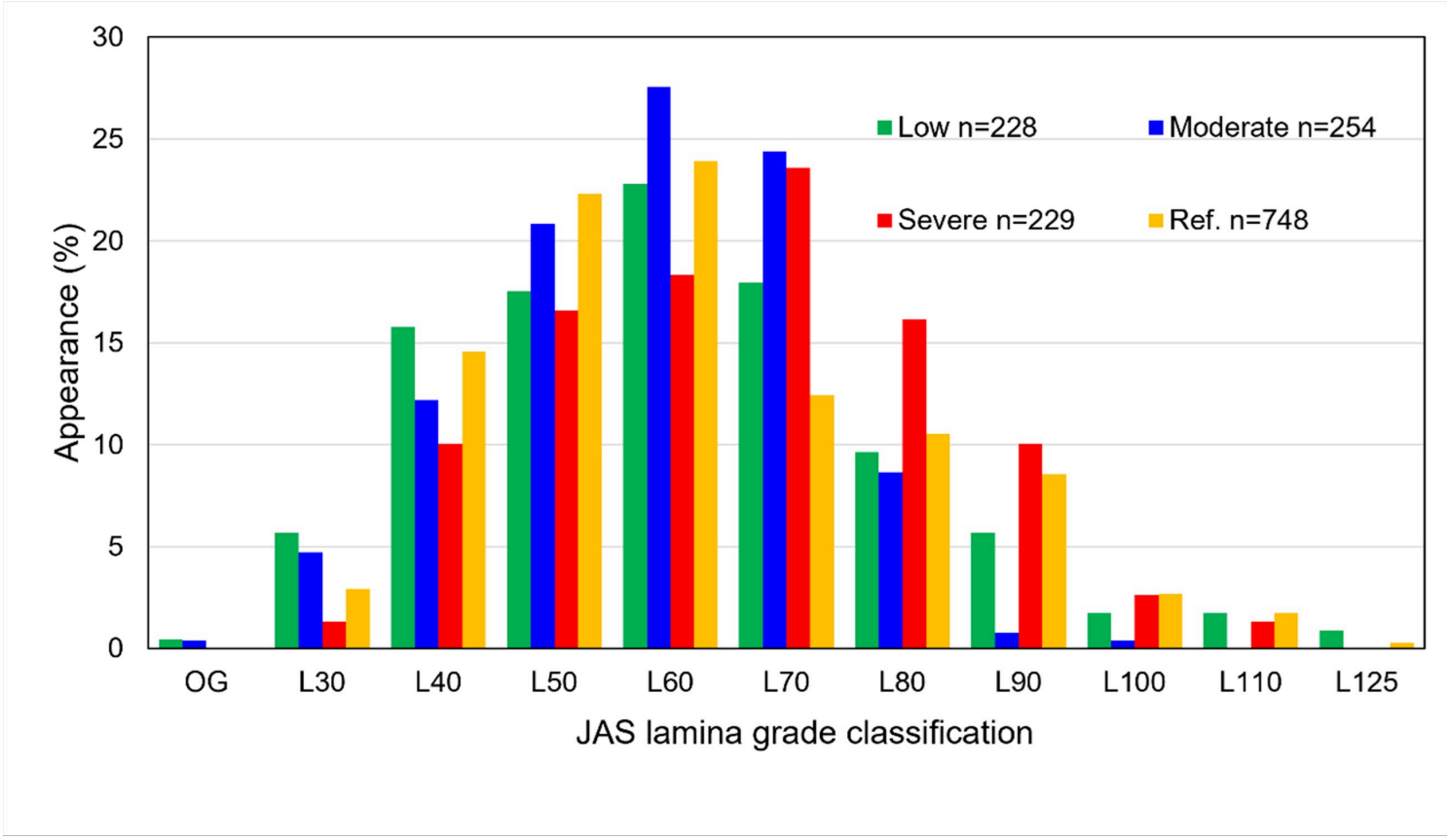


Figure 4

Distribution of JAS lamina grade classifications.

Percentage occurrence of laminae obtained from the low, moderate, and severe classes, compared with reference laminae.

The number of laminae was n = 228 for the low class, n = 254 for the moderate class, n = 229 for the severe class, and n = 748 for the reference group.

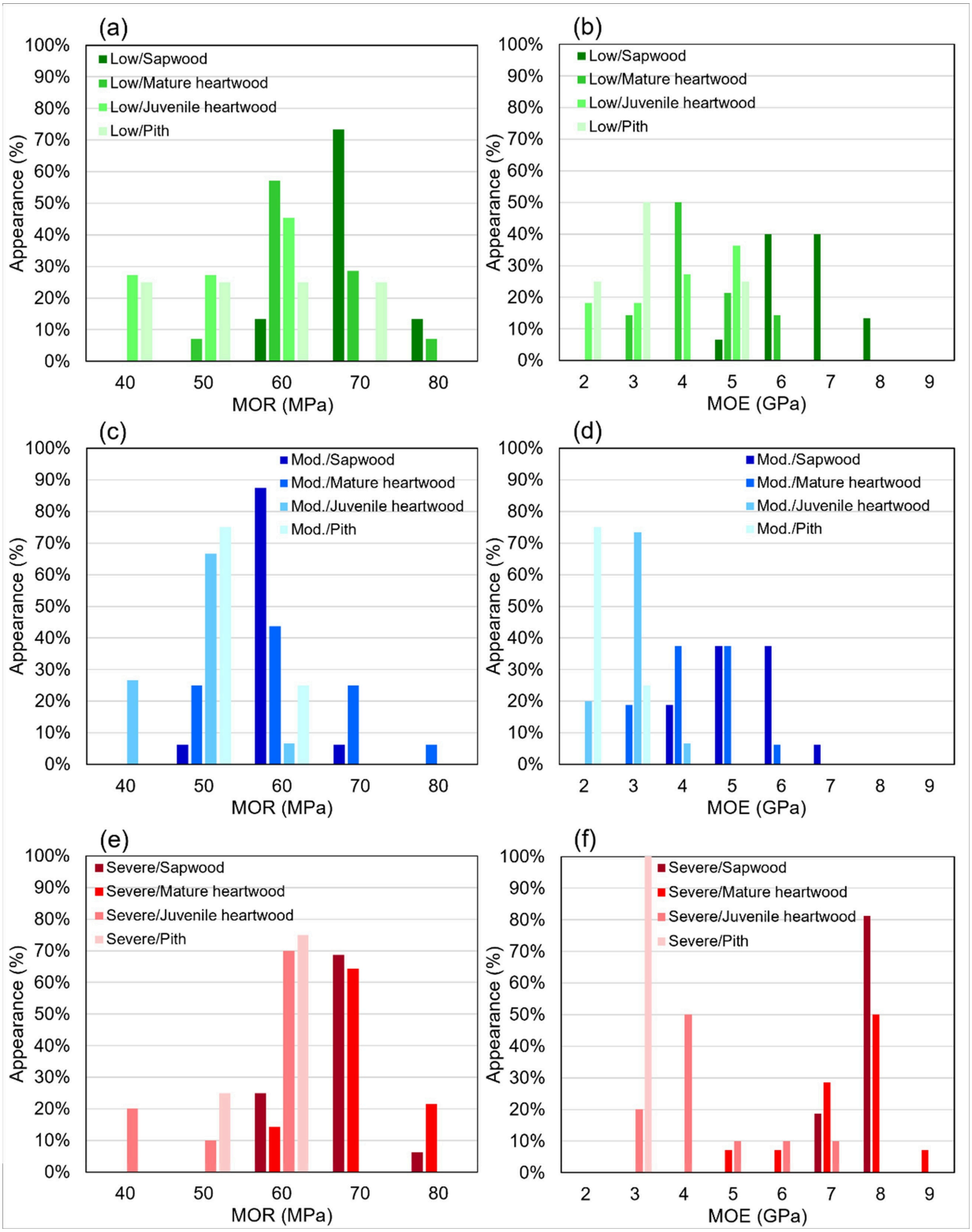


Figure 5

Effects of severity class and radial position on the distributions of MOR and MOE.

Distributions of modulus of rupture (MOR) and modulus of elasticity (MOE) are shown for the low class (a, b), moderate class (c, d), and severe class (e, f).

Within each severity class, specimens from sapwood, mature heartwood, juvenile heartwood, and the pith region were compared. The vertical axis indicates percentage occurrence within each radial-position group.

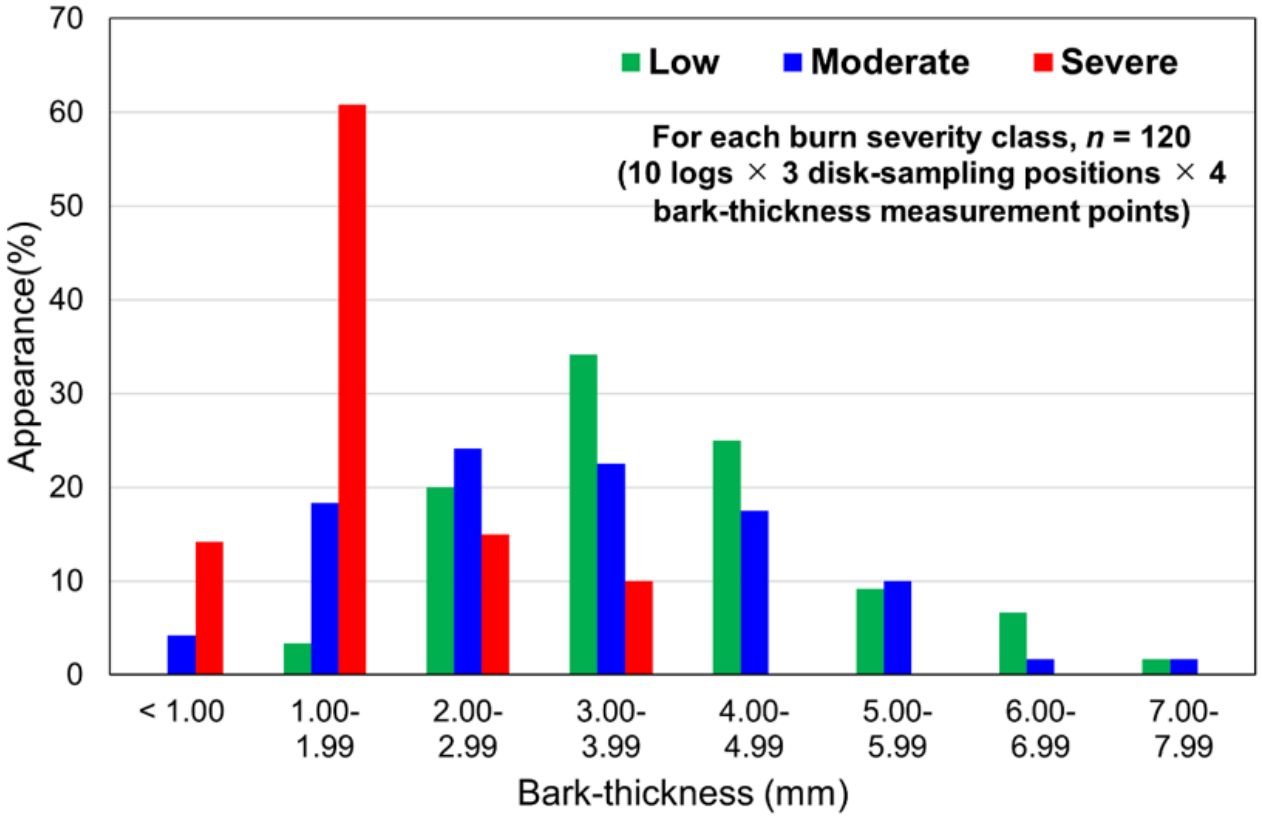


Figure 6

Percentage distribution of bark thickness in fire-damaged Cryptomeria japonica logs by burn severity class. Bark thickness was measured at three disk-sampling positions for 10 logs in each class, with four measurement points per disk (n = 120 per class).

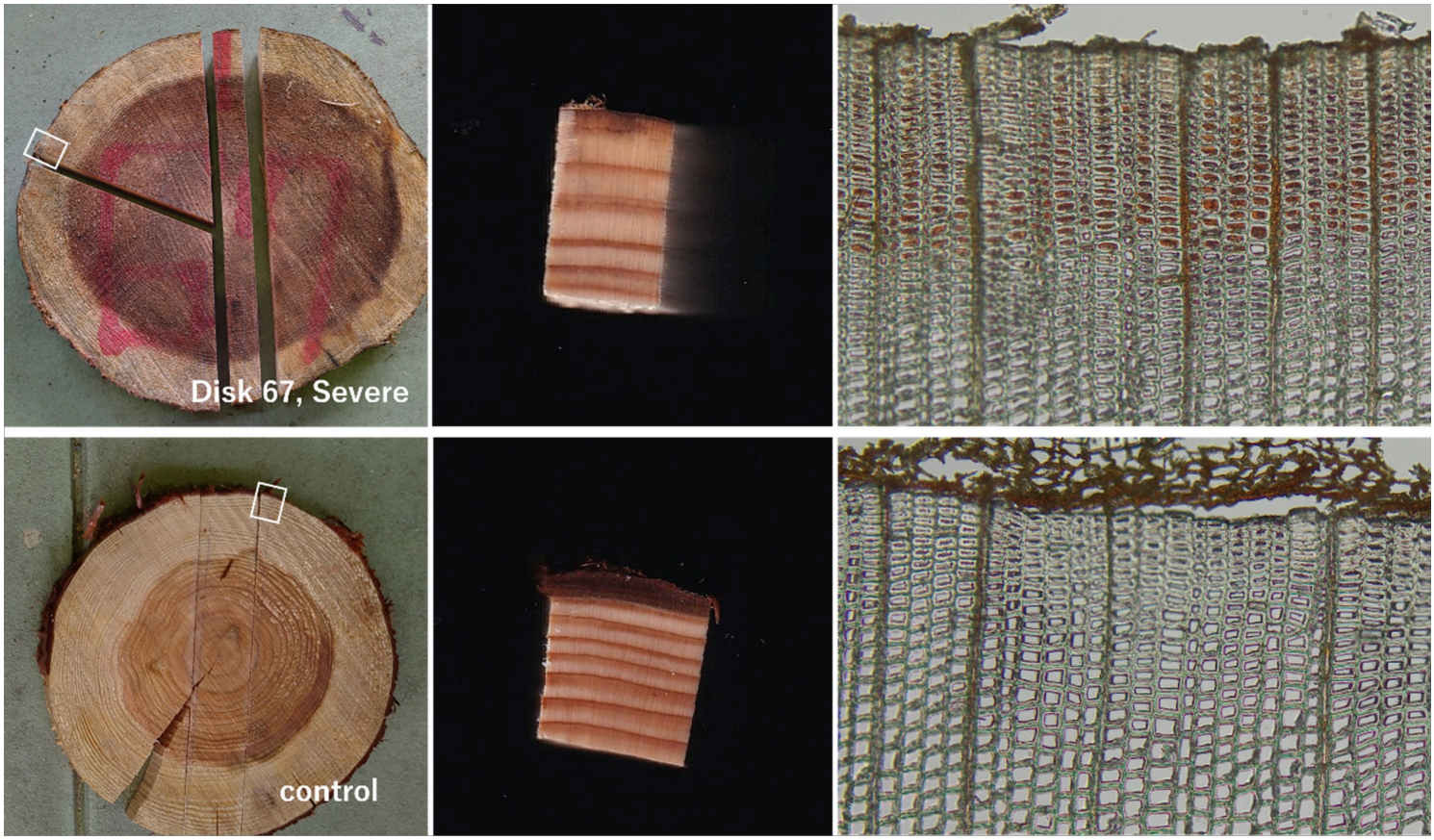


Figure 7

Macroscopic and microscopic observations of a severe-severity disk and a non-burned control disk.

The upper row shows the severe-severity sample, disk No. 67, and the lower row shows the non-burned control. The left column shows disk cross sections and sampling locations, the middle column shows small specimens excised from the indicated regions, and the right column shows transverse microscopic sections. White rectangles indicate the regions selected for microscopic observation.

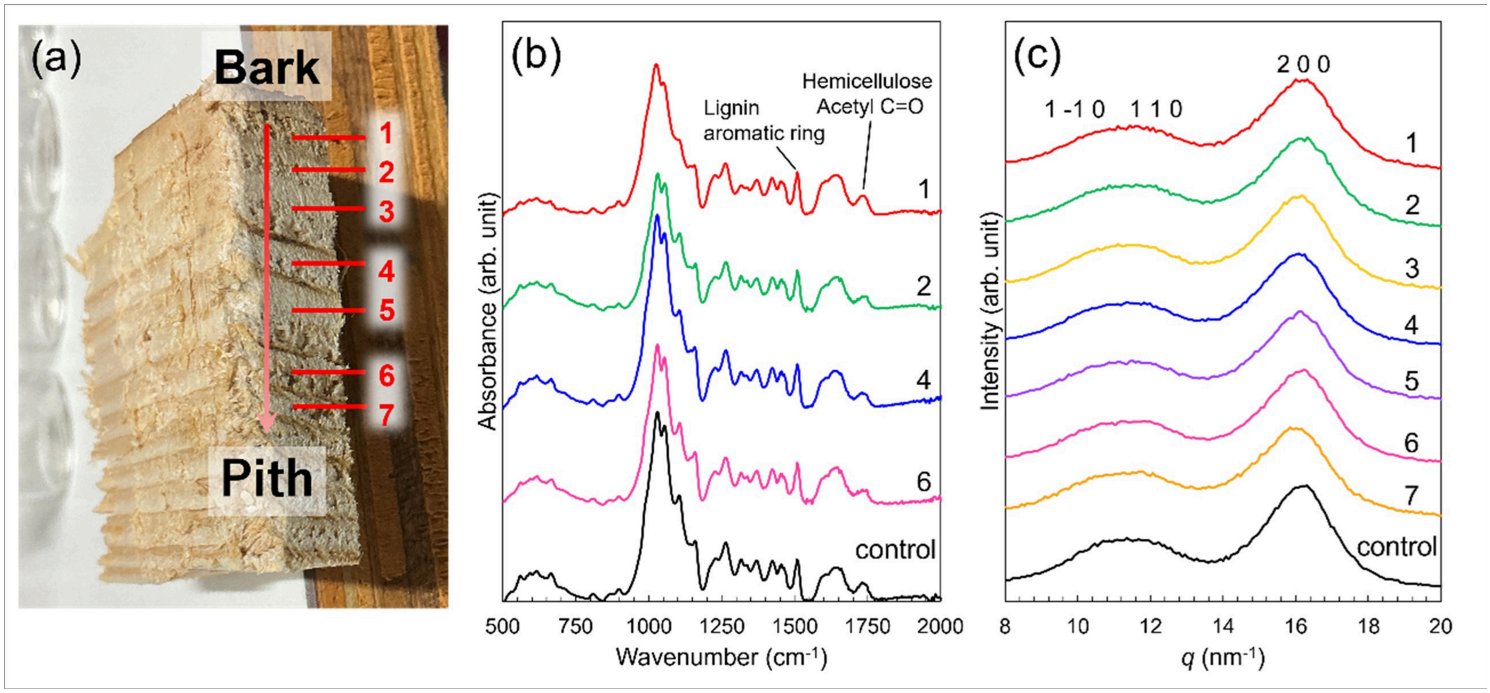


Figure 8

Radial sampling positions and spectroscopic/crystallographic profiles of the severe-severity sample.
(a) Annual-ring sampling positions in a radial strip prepared from the bark side toward the pith. The numbers and colors correspond to the FT-IR spectra and WAXD/XRD profiles shown in panels b and c. (b) FT-IR spectra used to evaluate the retention of characteristic functional groups of hemicellulose, cellulose, and lignin. (c) WAXD/XRD profiles used to evaluate the retention of cellulose Iβ crystalline structure.

Supplementary Files

This is a list of supplementary files associated with this preprint. Click to download.

- SupportingInformationsubmission.docx
- Graphicalabstract.png